

- [17] R. Fort, J. Favre und L. Deriwelle, *Bull. Soc. chim. France* 534 (1955).
 [18] M. M. Rochkind und G. C. Pimentel, *J. chem. Physics* 42, 1361 (1965).
 [19] R. H. Miller, D. L. Bernitt und I. C. Hisatsune, *Spectrochim. Acta A* 23, 223 (1967).
 [20] G. E. McGraw, D. L. Bernitt und I. C. Hisatsune, *J. chem. Physics* 42, 237 (1965).
 [21] J. D. Rogers, *J. chem. Physics* 34, 2195 (1961).
 [22] L. Bru, M. P. Rodriguez und M. Cubero, *J. chem. Physics* 20, 1069 (1952).
 [23] E. B. Wilson jr., I. C. Decius und P. C. Cross, *Molecular Vibrations*, McGraw-Hill Book Comp. Inc., New York 1955.
 [24] J. H. Schachtschneider und F. S. Mortimer, *Vibrational Analysis of Polyatomic Molecules V*, Techn. Rept. No. 231 bis 264, Shell Development Comp. Emeryville, Cal.

(Eingegangen am 18. Juli 1977, E 3753

endgültige Fassung am 5. September 1977)

Direct Rate Measurements for $\text{OH} + \text{OH} \rightarrow \text{H}_2\text{O} + \text{O}$ in the Range 1200–1800 K

J. Ernst, H. Gg. Wagner, and R. Zellner

Institut für Physikalische Chemie der Universität, 3400 Göttingen, West-Germany

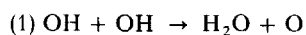
Freie Radikale / Reaktionskinetik / Resonanzabsorption / Stoßwellen

Rate constants for the disproportionation reaction (1) $\text{OH} + \text{OH} \rightarrow \text{H}_2\text{O} + \text{O}$ in the range $T = 1200\text{--}1800\text{ K}$ have been measured by a direct technique using shock heating of HNO_3/Ar mixtures as a source of a strongly non-equilibrated OH concentration and time resolved UV resonance absorption as its monitor. The result, $k_1 = 3.4 \cdot 10^{13} \exp(-21 \text{ kJ mol}^{-1}/RT) \text{ cm}^3/\text{mol} \cdot \text{s}$, does not correlate with the accepted absolute data at room temperature and implies that the Arrhenius plot for this reaction is strongly curved. It is shown that presently available data in the range $300\text{--}2000\text{ K}$ can be represented best by a $k = AT^m$ expression. Whereas an empirical interpolation based on the weighted absolute values of all rate constants yields $k_1 = 1.5 \cdot 10^9 (T/\text{K})^{1.14} \text{ cm}^3/\text{mol} \cdot \text{s}$, the result of a transition state theory calculation implies a slightly stronger temperature dependence ($k_1^{\text{TST}} = 6.6 \cdot 10^8 (T/\text{K})^{1.23} \text{ cm}^3/\text{mol} \cdot \text{s}$) with apparent Arrhenius activation energies of zero around room temperature and $\sim 20 \text{ kJ mol}^{-1}$ in the $1000\text{--}2000\text{ K}$ range.

Direkte Messungen der Geschwindigkeitskonstanten für die Disproportionierungsreaktion (1) $\text{OH} + \text{OH} \rightarrow \text{H}_2\text{O} + \text{O}$ wurden im Bereich $T = 1200\text{--}1800\text{ K}$ ausgeführt. Der thermische Zerfall von HNO_3 in Stoßwellen diente als Quelle für hohe Nicht-Gleichgewichts-Konzentrationen des OH-Radikals und zeitaufgelöste UV-Resonanzabsorption als dessen Nachweis. Das Ergebnis, $k_1 = 3.4 \cdot 10^{13} \exp(-21 \text{ kJ mol}^{-1}/RT) \text{ cm}^3/\text{mol} \cdot \text{s}$, korreliert nicht mit der akzeptierten absoluten Geschwindigkeitskonstante bei Zimmertemperatur, und es sagt eine starke Krümmung der Arrheniusauftragung für diese Reaktion voraus. Es wird gezeigt, daß alle bisher gemessenen Geschwindigkeitskonstanten im Bereich $T = 300\text{--}2000\text{ K}$ am besten durch einen Ausdruck der Form $k = AT^m$ dargestellt werden können. Während eine empirische Interpolation auf der Basis der gewichteten absoluten Geschwindigkeitskonstanten zu $k_1 = 1.5 \cdot 10^9 (T/\text{K})^{1.14} \text{ cm}^3/\text{mol} \cdot \text{s}$ führt, liefert die Anwendung der Theorie des Übergangszustandes (TST) eine leicht stärkere Temperaturabhängigkeit ($k_1^{\text{TST}} = 6.6 \cdot 10^8 (T/\text{K})^{1.23} \text{ cm}^3/\text{mol} \cdot \text{s}$) mit einer scheinbaren Arrhenius-Aktivierungsenergie von Null bei Zimmertemperatur und von $\sim 20 \text{ kJ mol}^{-1}$ im Bereich $1000\text{--}2000\text{ K}$.

Due to its outstanding importance in combustion systems the kinetics of hydroxyl radical reactions has received considerable attention. Literature data up to 1969 have been critically reviewed by the Leeds group [1]. In subsequent years rate data for a number of important hydroxyl radical reactions have been considerably refined, in particular at temperatures below 1000 K , where these reactions can be studied in isothermal flow or static systems with sensitive OH detection techniques. By way of contrast rate data for temperatures above 1000 K are still lacking a sufficient degree of accuracy, mainly due to the complexity of kinetic systems from which rate data for an individual process have to be extracted and also by a severe loss of detection sensitivity. The need of high temperature data is further provoked by the experimental observation in some system of non-Arrhenius behaviour which does no longer allow simple exponential extrapolation.

The present work presents results of a direct investigation of the disproportionation reaction



in the range $T = 1200\text{--}1800\text{ K}$. So far similar (direct) measurements have only been reported for room temperature [2–9]. These data together with direct measurements of the reverse reaction in the range $750\text{--}1050\text{ K}$ by Albers et al. [10] have lead to an accepted Arrhenius activation energy of 4.6 kJ/mol from $300\text{--}1000\text{ K}$. Recently, however, Rawlins and Gardiner [11], following a previous publication [12], have presented evidence that the apparent activation energy for this reaction above 1000 K is much larger, $E_A \approx 29 \text{ kJ/mol}$.

In view of being faced with either a strong discrepancy or a genuine case of non-Arrhenius behaviour, we have undertaken a direct investigation of this reaction at high temperatures. Our experiments were carried out behind reflected

shock waves utilizing the thermal decomposition of HNO_3 as a source for OH and time resolved OH ($A^2\Sigma^+ - X^2\Pi$) resonance absorption as its monitor. Such a system can produce strongly non-equilibrated OH concentrations in the absence of any relevant concentration of other OH removing species and its decay in reaction (1) can be studied directly.

Due to its kinetic simplicity we feel that such a system is in this particular respect, advantageous to shock-heated H_2/O_2 mixtures and the extraction of kinetic data from induction zone or pre-partial equilibrium 'spikes' in the OH profile [11]. Because of insufficient detection sensitivity for OH, however, the HNO_3 source can hardly be recommended for the study of other OH reactions. We will, however, in a forthcoming paper [13] report a new flash photolysis/shock tube combination where the decay of OH in the presence of other reactants (i.e. CH_4) is monitored following rapid equilibration of OH in shock heated and flash photolysed $\text{H}_2\text{O}/\text{Ar}$ mixtures.

Experimental

The experimental set up of the shock tube experiment and the extraction of the physical properties of the shock front have been described previously [14]. The concentration of OH was recorded behind the reflected shock wave, 4.5 cm from the end plate. OH resonance radiation in the ($A^2\Sigma^+ - X^2\Pi$) system was provided by a microwave powered discharge of H_2O vapour in Ar. In order to obtain an enhanced path length, this radiation was reflected twice by means of a simple mirror system. In this way 3 traversals across the shock tube and an effective absorption path length of 30 cm were obtained before the radiation was focussed onto the slit of a prism monochromator (Zeiss MQ 4 III) centered at 308 nm. Radiation intensities were monitored with a photomultiplier (EMI 6256 A) and were displayed on a storage oscilloscope. Using an anode load resistance of 50 k Ω , the detection response constant was 5 μs , sufficient small compared to average time constants for the decay of OH of 400 μs .

In order to obtain a satisfactory signal to noise ratio, which is further reduced due to a loss of total intensity in the multiple pass arrangement, we have chosen a large spectral band width ($\Delta\lambda \approx 10 \text{ nm}$). Although in this arrangement the rotational structure of the (0,0) band of OH is completely unresolved, we are still dealing with multiple line absorption and with a detection sensitivity not very much different from a single line absorption experiment. This is because the rotational temperature of the OH source lamp is very much lower ($T \sim 640 \text{ K}$) than the absorber temperature and therefore the lines with higher K values, which would preferentially be used in a single line absorption experiment at higher temperatures, are emitted less strongly. Moreover the full band absorption experiment is expected to create less temperature dependence of the effective absorption coefficient. Due to the non-uniform value of the line absorption coefficients over the incident spectral interval and the relatively large optical densities, however, the absorption is not expected to increase linearly with $[\text{OH}]$, i.e. to follow the Beer-Lambert law. We have therefore chosen to employ the usual modification,

$$\ln(I_0/I) = \varepsilon_{\text{eff}}([\text{OH}] \cdot l)^\gamma$$

where γ can be assumed a constant over a certain range of $[\text{OH}]$. The value of γ for our experimental arrangement was determined by relating the initial OH absorption in shock-heated HNO_3/Ar mixtures to $[\text{HNO}_3]_0$, which under conditions of complete dissociation and uni-modal fragmentation [15] is equal to $[\text{OH}]_0$. From experiments using the same initial HNO_3/Ar mixture which was successively diluted in at least 5 separate runs, and plots of $\ln(\ln I_0/I)$ vs. $\ln([\text{OH}]_0 \cdot l)$, consistent values of $\gamma = 0.7 \pm 0.1$ independent upon temperature, were obtained. Due to difficulties

in reproducing the initial HNO_3 concentration in the Aluminium shock tube, experiments performed with different starting mixtures resulted in plots with the same slope (and, hence, the same value of γ) but different intercepts. This method was therefore unsuitable to determine the effective absorption coefficient.

Absolute Determination of the OH Concentration

In view of our second order kinetic analysis an accurate determination of the absolute OH concentration is essential. Since the above described HNO_3 technique has failed as a simple OH calibration procedure, we have chosen to determine the effective absorption coefficient from OH absorptions observed in partially equilibrated $\text{H}_2/\text{O}_2/\text{Ar}$ mixtures. Experiments were performed for H_2/O_2 concentrations between $(2-14) \cdot 10^{-9} \text{ mol cm}^{-3}$ at total densities of $\text{Ar} \approx 2 \cdot 10^{-5} \text{ mol cm}^{-3}$. The temperature range covered was 1360–2180 K. Partial equilibrium OH concentration for all experimental conditions were derived by numerical integration of the following reaction scheme

- (a) $\text{H}_2 + \text{Ar} \rightleftharpoons 2\text{H} + \text{Ar}$
- (b) $\text{O}_2 + \text{Ar} \rightleftharpoons 2\text{O} + \text{Ar}$
- (c) $\text{H}_2 + \text{O}_2 \rightleftharpoons 2\text{OH}$
- (d) $\text{H} + \text{O}_2 \rightleftharpoons \text{OH} + \text{O}$
- (e) $\text{O} + \text{H}_2 \rightleftharpoons \text{OH} + \text{H}$
- (f) $\text{OH} + \text{H}_2 \rightleftharpoons \text{H}_2\text{O} + \text{H}$
- (1) $\text{OH} + \text{OH} \rightleftharpoons \text{H}_2\text{O} + \text{O}$
- (g) $\text{H} + \text{O}_2 + \text{Ar} \rightleftharpoons \text{HO}_2 + \text{Ar}$
- (h) $\text{HO}_2 + \text{H}_2 \rightleftharpoons \text{H}_2\text{O} + \text{OH}$
- (i) $\text{H} + \text{OH} + \text{Ar} \rightleftharpoons \text{H}_2\text{O} + \text{Ar}$

The rate constants used in our computation were those employed in similar calculation by other authors [11, 16] previously, except that we have chosen k_1 according to our own preliminary results, approximately 20% larger than the expression of [11]. The result of $[\text{OH}]_{\text{eq}}$ is not very sensitive to the exact choice of k_1 since the partial equilibrium is largely determined by the branching reactions (d)–(f) [17]. The same is true for reactions (g)–(i). Their exclusion from the mechanism does not alter the result to an appreciable extent.

Fig. 1 is a plot of the observed absorption versus optical density, calculated from the partial equilibrium OH concentration. The data points included in this plot refer to absorption up to 32%. Most of them have been obtained from equimolar H_2/O_2 mixtures with the exception of data points (\odot) which are for a H_2/O_2 mixture of 13:1. A least squares fit yields a Beer-Lambert coefficient of $\gamma = 0.74$ in good agreement with the value determined independently from the HNO_3 calibration (see above).

The effective absorption coefficient (ε_{eff}) can now be obtained from an extrapolation of this plot. The intercept yields $\ln \varepsilon = 12.0 \pm 0.4$, and $\varepsilon_{\text{eff}} = 1.6 \cdot 10^5 \text{ cm}^2/\text{mol}$, which for 10% absorp-

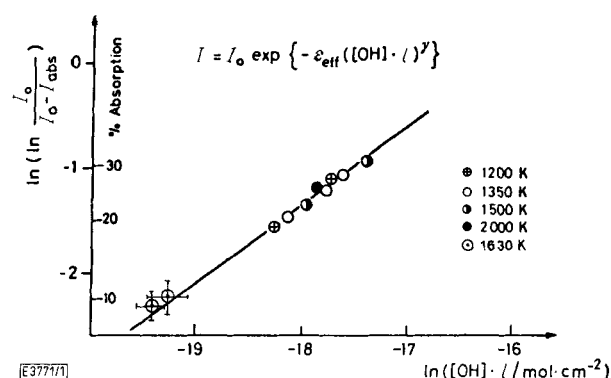


Fig. 1

Modified Beer-Lambert law analysis of observed OH absorption in shock heated $\text{H}_2/\text{O}_2/\text{Ar}$ mixtures. Partially equilibrated OH concentration are deduced by numerical integration of the reaction scheme (see text)

tion corresponds to an OH concentration of $1.4 \cdot 10^{-10} \text{ mol cm}^{-3}$ in our experimental arrangement ($l = 30 \text{ cm}$). It is to be noted that the data points in Fig. 1 refer to different temperatures in the range 1360–2180 K. However, γ (and by implication ϵ_{eff}) do not seem to show a systematic variation with temperature. We attribute this to our multiple line resonance absorption experiment. The simultaneous detection of absorption intensities on many lines of different K levels 'integrates' over the temperature dependent single lines absorptions on the expense of less total sensitivity. Whereas for a single Q₁3 line absorption at 1500 K we calculate for a 10% absorption in a 10 cm path length an OH concentration of $2.5 \cdot 10^{-10} \text{ mol cm}^{-3}$, we find here under conditions of multiple line absorption a corresponding OH concentration of $4.2 \cdot 10^{-10} \text{ mol cm}^{-3}$.

Materials

Nitric acid was prepared by mixing HNO₃ (Merck, suprapur) with concentrated sulphuric acid (Merck, suprapur) at 273 K. The flask with this mixture was then evacuated to $\sim 15 \text{ Torr}$ (vapour pressure of HNO₃ at 273 K) and HNO₃ was distilled into a trap at 77 K. This sample was then distilled 3 times from 195 K to 77 K. HNO₃ was obtained as a colourless liquid and was stored in the dark at 77 K. All gas mixtures to be used in the shock tube were made up in a glass bulb. The partial pressures were measured with a mercury gauge. The gases used had the following stated purities: H₂: 99.9996%, O₂: 99.9996%, Ar: 99.997%. NO₂ was taken from a cylinder (Matheson Co.) and was purified by repeated distillation.

Results

Reaction (1) has been studied in the range $T = 1180\text{--}1820 \text{ K}$ by monitoring the decay of OH following the instantaneous decomposition of HNO₃ in shock heated HNO₃/Ar mixtures. A typical experimental result is shown in Fig. 2. Such traces, if analyzed in second-order kinetics using the relation

$$l \cdot \left\{ \exp \left[\frac{\ln(I_0/I) - \ln \epsilon_{\text{eff}}}{\gamma} \right] \right\}^{-1} = nk_1 \cdot t$$

where $l = 30 \text{ cm}$, the absorption path length, I_0 and I the incident and transmitted intensities (at time t), and ϵ_{eff} and γ as defined above,

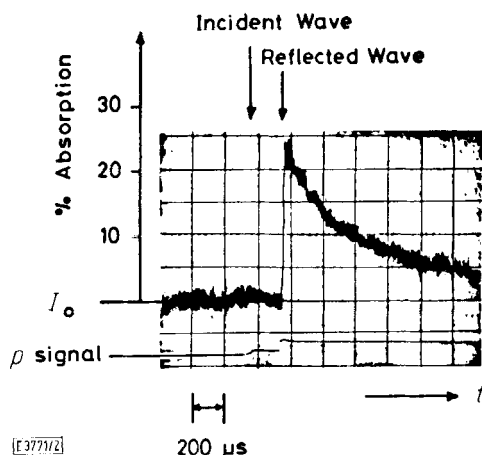
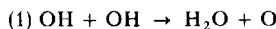


Fig. 2

Experimental trace of OH-UV absorption in shock heated HNO₃/Ar mixtures. $T = 1350 \text{ K}$; $[\text{Ar}] \approx 2 \cdot 10^{-5} \text{ mol/cm}^3$; $[\text{HNO}_3]_0 \approx 5 \cdot 10^{-10} \text{ mol/cm}^3$. The peak absorption of 23% corresponds to $[\text{OH}]_0 = [\text{HNO}_3]_0$. (The trace labeled 'p signal' is the output from a pressure transducer)

always resulted in straight lines, with a slope of nk_1 . This is supporting evidence that the reaction

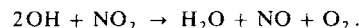


is the dominant decay process. According to the results [15] on the thermal decomposition of HNO₃ the time constant for the decay of HNO₃ under our conditions is always $< 10 \mu\text{s}$, so that no interference of the OH profile from successive OH formation should be expected.

In order to extract from the observed decay the rate constant k_1 , the factor n in the above rate law has to be carefully analyzed. We have carried out a numerical analysis of our reaction sequence incorporating the following reactions which may be initiated in the presence of NO₂ and from the products of reaction (1):

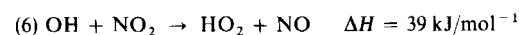
- (2) $\text{O} + \text{OH} \rightarrow \text{O}_2 + \text{H}$
- (3) $\text{O} + \text{NO}_2 \rightarrow \text{O}_2 + \text{NO}$
- (4) $\text{H} + \text{NO}_2 \rightarrow \text{OH} + \text{NO}$
- (5) $\text{H} + \text{H}_2\text{O} \rightarrow \text{OH} + \text{H}_2$

The result shows that reaction (2) indeed occurs and would tend to increase the stoichiometric factor n to larger than 2.0, the value imposed from reaction (1) only. However, this effect is drastically reduced through the presence of NO₂. Firstly, a large amount of oxygen atoms is channeled into reaction (3) and, secondly, the consumption of OH in reaction (2) is fully compensated by its fast regeneration in reaction (4). Finally, reaction (5) remains unimportant because of the low steady state H atom concentration. The total reaction stoichiometry may therefore under the conditions of our experiments be formulated as



Taking the rate constants $k_2 - k_5$ from the literature (k_2, k_3 from [1], k_4 from [18] and k_5 from [19]) the computed OH profile does agree with the experimental one to within 3% for a stoichiometric factor of $n = 2$.

The completeness of the consecutive reactions involving NO₂ has been further tested by deliberately adding NO₂ to the initial HNO₃/Ar mixtures. For NO₂ concentrations up to two times the initial HNO₃ concentration, no further reduction of nk_1 was observed. It should be added that over the whole range of our experiments a direct reaction between OH and NO₂



(which is expected to have an activation energy of at least 40 kJ mol⁻¹), as well as thermal dissociation of NO₂ will be too slow to interfere with the above mentioned scheme to an appreciable extent.

Rate constants $k_1 = -d[\text{OH}]/(2[\text{OH}]^2 \cdot dt)$ over the temperature range $T = 1180\text{--}1820 \text{ K}$ are presented in Arrhenius form in Fig. 3. A least squares treatment of the data yields the expression:

$$k_1 = 3.4 \cdot 10^{13} \exp(-21 \text{ kJ mol}^{-1}/RT) \text{ cm}^3/\text{mol} \cdot \text{s}$$

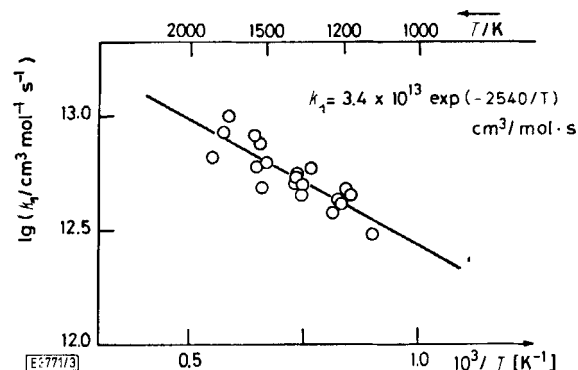


Fig. 3

Arrhenius plot of the rate constants k_1 as obtained in this work

Discussion

i) Comparison with Previous Measurements

Previous measurements of k_1 fall into two categories: a) a large number of room temperature investigations, mostly in discharge-flow systems [2–8] except one study [9] by a static flash photolysis technique, and b) one high temperature shock tube investigation [11, 12] of the H_2/O_2 reaction. No measurements on reaction (1) have so far been reported in the intermediate range. In their evaluation in 1971, Baulch et al. [1] have used the weighted average room temperature rate constant $k_1 = 1.0 \cdot 10^{12} \text{ cm}^3/\text{mol} \cdot \text{s}$ together with the (at that time) only dependable high temperature data by Albers et al. [10] (a discharge-flow system study on the reverse of reaction (1)) to deduce an Arrhenius activation energy of $4.6 \pm 1.7 \text{ kJ mol}^{-1}$. Recently, Rawlins and Gardiner [11] have presented evidence of a much larger activation energy at high temperatures. From an analysis of OH 'spike' profiles prior to the attainment of quasi-equilibrium in shock-heated $\text{H}_2/\text{O}_2/\text{Ar}$ mixtures, the authors deduce an apparent Arrhenius activation energy for reaction (1) of 29 kJ mol^{-1} in the range 1500 to 2000 K. Their absolute data could be reconciled with both, the room temperature results and the data by [10] on the reverse reaction, if non-Arrhenius behaviour and an additional T^n factor in the temperature dependent rate expression were assumed. Fig. 4 is an Arrhenius plot of low and high temperature rate constants for reaction (1), including the result from the present work. Our data virtually confirm the results of [11]. There is good agreement between the two sets of data; the rate constants on the high temperature end being essentially identical ($k_1(2000 \text{ K}) \approx 9 \cdot 10^{12} \text{ cm}^3/\text{mol} \cdot \text{s}$). However, the temperature dependence found in our study is slightly less pronounced ($E_A = 21 \text{ kJ mol}^{-1}$). This difference should not be overestimated in view of the scatter in both experiments. However, since our results were obtained by a direct technique we attribute to them a somewhat larger reliability.

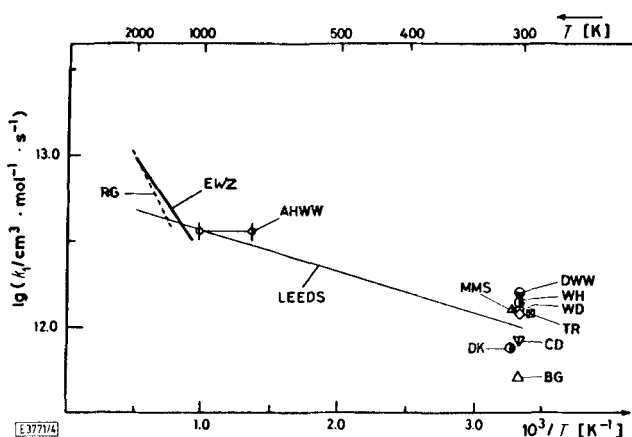


Fig. 4

Arrhenius plot of reported rate constants for the reaction $\text{OH} + \text{OH} \rightarrow \text{H}_2\text{O} + \text{O}$. DK: Del Greco, Kaufman [2], WH: Westenberg, de Haas [3], DWW: Dixon-Lewis et al. [4], WD: Wilson, O'Donovan [5], BG: Breen, Glass [6], AHW: Albers et al. [10] (from reverse reaction and using the equilibrium constant from [20]), LEEDS: Baulch et al. [1], MMS: McKenzie et al. [7], TR: Trainor, von Rosenberg [9], CD: Clyne, Down [8], RG: Rawlins, Gardiner [11], EWZ: this work

Moreover, our data are also compatible with the Albers et al. [10] result on the reverse $\text{O} + \text{H}_2\text{O}$ reaction. Converting their absolute data at 1000 K with the equilibrium constant from JANAF tables [20] a rate constant k_1 is obtained which is only about 40% larger than the present result.

Our rate constant expression, however, does not extrapolate to the room temperature measurements. Although there is still some disagreement between these data (even results obtained within the last 5 years with well established techniques differ by a factor of 2), it is inconceivable that they can be correlated with our high temperature results in terms of one single Arrhenius expression. Following the experimentally established observations of curved Arrhenius behaviour in other reactions of the hydroxyl radical (i.e. $\text{OH} + \text{CO}$ [21], $\text{OH} + \text{CH}_4$ [22] and $\text{OH} + \text{H}_2$ [23]) and in accordance with [11] we chose to represent the temperature dependence in form of a $k = AT^m$ expression. The result, $k_1 = 1.5 \cdot 10^9 \cdot T^{1.14} \text{ cm}^3/\text{mol} \cdot \text{s}$ is included in Fig. 4. We feel that such an expression gives the best account of all data so far available. It should be noted, however, that its parameter may have to be altered, once the room temperature rate constant becomes more accurately defined or direct rate measurements in the intermediate temperature range become available. Such measurements are under way in this laboratory.

ii) Transition State Theory Calculation

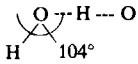
The non-linear behaviour of Arrhenius graphs has so far been lacking a concise understanding [24]. Its possible explanation in terms of the participation of vibrationally excited states of one or both reactant molecules [25] could, at least in some cases, not be confirmed by direct studies of vibrational enhancement of OH reactions [26]. It could, however, quite successfully be reproduced by application of transition state theory (TST) which is a formal concept of a temperature dependent 'activation energy'.

For the reaction under consideration the room temperature rate constant is defined to within $\pm 50\%$ limits as $1 \cdot 10^{12} \text{ cm}^3/\text{mol} \cdot \text{s}$. There is no direct experimental evidence as to the magnitude of the Arrhenius activation energy around room temperature. The task of a TST calculation is therefore to combine a room temperature fix point with temperature dependent data at $> 1000 \text{ K}$. In our calculation we have used a 4-atomic non-linear transition state model with assumed fully active rotations. The vibrational analysis of this complex was made by the BEBO method [27] for the central (linear) $\text{O}-\text{H}-\text{O}$ configuration, whereas the additional bending frequency around $\angle \text{HOH}$ was taken as the bending frequency in the H_2O molecule [28] multiplied by the square root of the $\text{HO}-\text{H}$ bond order in the complex. Rate constants were finally calculated from the expression

$$k(T) = \frac{C}{T} \cdot \frac{Q_{\text{vib}}^{\ddagger}}{Q_{\text{vib,OH}}} \exp(-V^*/RT)$$

where C/T accounts for translational and rotational partition functions and their temperature dependence as well as the kT/h term; Q_{vib} being the product of 4 vibrational partition functions (one OHO symmetric stretch, two (degenerate)

Table 1
Model and properties of transition state for the reaction
 $\text{OH} + \text{OH} \rightarrow \text{H}_2\text{O} + \text{O}$

4-atomic model:			
$r_{\text{O-H}}^*/\text{\AA}$	1.14	ν^* (O-H-O asym. stretch)	reaction coordinate
$r_{\text{H-O}}^*/\text{\AA}$	1.14	ν_1 (O-H-O sym. stretch)	648 cm^{-1}
$V^*/\text{kJ mol}^{-1}$	7.94	ν_2 (O-H-O bend)	348 cm^{-1}
$E_{\text{A}}^{300}/\text{kJ mol}^{-1}$	0.26	ν_3 (H-O-H bend)	1128 cm^{-1}
$(p = q)$	0.999)	the O-H stretch frequency $\nu_4 = 3735 \text{ cm}^{-1}$ was assumed the same in the complex and reactant	

OHO bends, one HOH bend) and $Q_{\text{vib,OH}}$ is the OH vibrational partition function. V^* is the classical energy barrier and available from a BEBO calculation. The constant C is adjusted such that agreement with the accepted experimental rate constant at 300 K is obtained.

The results of our calculation can be summarized as follows: Using the input data for the BEBO calculation from Johnston [27] with no further adjustments, rate constants at temperatures above 1000 K were predicted, that were much too large. This is because the calculation predicts a (positive) room temperature activation energy of $\sim 10 \text{ kJ/mol}$ and this positive temperature coefficient is further enhanced by the temperature dependence of the vibrational partition function, which outweighs quickly the T^{-1} term. This result is independent upon whether the BEBO calculation is done with a symmetrical potential (assigning the same energy to the ruptured and the newly formed O-H bond) or an asymmetric potential in which the O-H bond energy differences in OH and H_2O are accounted for.

In view of this apparent failure we have decided to treat the BEBO bond energy index as adjustable. It should be noted that the physical justification for an re-evaluation of this parameter has been considered in two recent publications [29, 30]. The input parameters used and the bond energy index that gave agreement with the experimental data are summarized in Table 1. The result for $k(T)$ is also presented

graphically in Fig. 5. The predicted activation energy in the temperature range 1200–2000 K is $\sim 20 \text{ kJ/mol}$. Moreover, the calculated result implies that the apparent activation energy around room temperature is very close to zero. The analytical form of $k(T)$ obtained here can be represented by

$$k(T) = 6.6 \cdot 10^8 \cdot (T/\text{K})^{1.23} \text{ cm}^3/\text{mol} \cdot \text{s}.$$

Finally it should be noted, that due to a bond energy index of nearly unity the potential energy barrier V^* is almost entirely due to the end atom triplet repulsion, which is the most arbitrary part of the theory. We therefore regard the result as of more descriptive rather than predictive nature.

Financial support of this work by 'Fonds der Chemischen Industrie' is gratefully acknowledged. One of us (R.Z.) thanks NATO for the award of a research grant.

References

- [1] D. L. Baulch, D. D. Drysdale, D. G. Horne, and A. C. Lloyd, Evaluated Kinetic Data for High Temperature Reactions, Vol. 1, Butterworths, London 1972.
- [2] F. P. Del Greco and F. Kaufman, Discuss. Faraday Soc. 33, 128 (1962).
- [3] A. A. Westenberg and N. de Haas, J. chem. Physics 43, 1550 (1965); 58, 4066 (1973).
- [4] G. Dixon-Lewis, W. E. Wilson, and A. A. Westenberg, J. chem. Physics 44, 2877 (1966).
- [5] W. E. Wilson and J. T. O'Donovan, J. chem. Physics 47, 5455 (1967).
- [6] J. E. Breen and G. P. Glass, J. chem. Physics 52, 1082 (1970).
- [7] A. McKenzie, M. F. R. Mulcahy, and J. R. Steven, J. chem. Physics 59, 3244 (1973).
- [8] M. A. A. Clyne and S. Down, J. chem. Soc. Faraday II 70, 253 (1974).
- [9] D. W. Trainor and C. W. von Rosenberg, Jr., J. chem. Physics 61, 1010 (1974).
- [10] E. A. Albers, K. Hoyermann, H. Gg. Wagner, and J. Wolfrum, XIIIth Symp. (Int.) on Combustion, 81 (1971).
- [11] W. T. Rawlins and W. C. Gardiner, Jr., J. chem. Physics 60, 4676 (1974).
- [12] W. C. Gardiner, Jr., K. Morinaga, D. L. Ripley, and T. Takeyama, J. chem. Physics 48, 1665 (1968).
- [13] J. Ernst, H. Gg. Wagner, and R. Zellner, Ber. Bunsenges. physik. Chem., to be published.
- [14] E. F. Greene and J. P. Tonnies, Chemical Reactions in Shock Waves, E. Arnold, London 1964; W. Jost, K. W. Michel, J. Troe, and H. Gg. Wagner, Z. Naturforsch. 19a, 59 (1964).
- [15] K. Glänzer and J. Troe, Ber. Bunsenges. physik. Chem. 78, 71 (1974).
- [16] J. N. Bradley, W. D. Capey, R. W. Fair, and D. K. Pritchard, Int. J. chem. Kin. 8, 549 (1976).

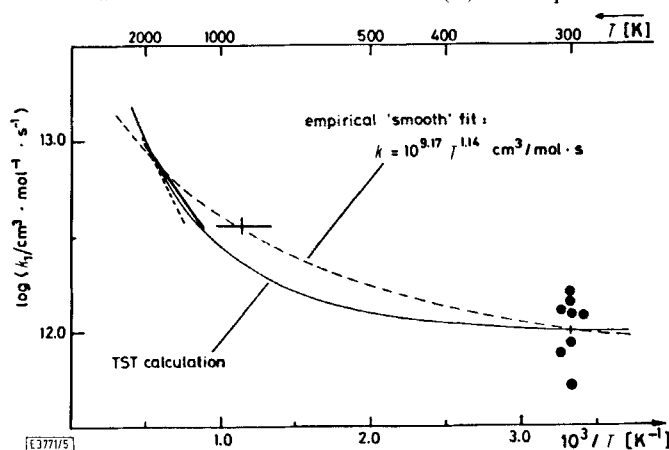


Fig. 5

'Smoothed' Arrhenius plot for the reaction $\text{OH} + \text{OH} \rightarrow \text{H}_2\text{O} + \text{O}$. The dashed line is an empirical AT^m -fit based on the weighted average absolute rate constants (at $T = 300 \text{ K}$ and the results of [10], [11] and of this work). The solid line represents the result from a transition state theory calculation, details of which are described in the text

- [17] G. L. Schott, *J. chem. Physics* **32**, 710 (1960).
 [18] D. L. Baulch, D. D. Drysdale, D. G. Horne, and A. C. Lloyd, *Evaluated Kinetic Data for High Temperature Reactions*, Vol. 2, Butterworths, London.
 [19] H. Gg. Wagner, U. Welzbacher, and R. Zellner, *Ber. Bunsenges. physik. Chemie* **80**, 1023 (1976).
 [20] JANAF Thermochemical Tables, US Department of Commerce, National Bureau of Standards, 1972.
 [21] D. L. Baulch and D. D. Drysdale, *Comb. Flame* **23**, 215 (1974); I. W. M. Smith and R. Zellner, *J. chem. Soc. Faraday II* **69**, 1617 (1973).
 [22] R. Zellner and W. Steinert, *Int. J. chem. Kin.* **8**, 397 (1976).
 [23] W. C. Gardiner, Jr., W. G. Mallard, and J. H. Owen, *J. chem. Physics* **60**, 2290 (1974).
 [24] For a recent account of non-Arrhenius behaviour see W. C. Gardiner, Jr., *Accounts Chem. Res.*, in press.
 [25] W. C. Gardiner, Jr., W. G. Mallard, M. McFarland, K. Morinaga, J. H. Owen, W. T. Rawlins, T. Takeyama, and B. F. Walker, *XIVth Symp. (Int.) on Combustion*, **61** (1973).
 [26] J. E. Spencer, H. Endo, and G. P. Glass, *XVIth Symp. (Int.) on Combustion*, to be published 1977.
 [27] H. S. Johnston, *Gas Phase Reaction Rate Theory*, The Ronald Press Co., New York 1966.
 [28] G. Herzberg, *Infrared and Raman Spectra of Polyatomic Molecules*, Van Nostrand Co.
 [29] R. M. Jordan and F. Kaufman, *J. chem. Physics* **63**, 1691 (1975).
 [30] R. D. Gilliom, *J. chem. Physics* **65**, 5027 (1976).

(Eingegangen am 11. August 1977) E 3771

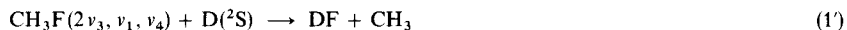
Reaktionen von Molekülen in definierten Schwingungszuständen (V), Schwingungsangeregte mehratomige Moleküle im Elektronengrundzustand: $\text{CH}_3\text{F}(2\nu_3, \nu_1, \nu_4) + \text{D}(^2\text{S}), \text{O}(^3\text{P})^*$

M. Kneba und J. Wolfrum

Max-Planck-Institut für Strömungsforschung, D-3400 Göttingen, Germany

Chemische Bindung / Energieübertragung / Fluoreszenz / Photochemie / Reaktionskinetik

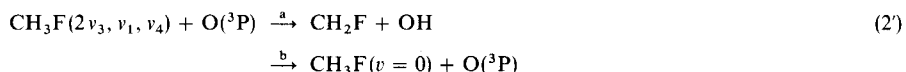
Der Einfluß einer selektiven Schwingungsanregung auf das Reaktionsverhalten mehratomiger Moleküle in der Gasphase wurde für die Reaktionen von $\text{CH}_3\text{F}(v)$ mit H-, D- und O-Atomen mit Hilfe der Methode der laserinduzierten Fluoreszenz in einem Strömungsreaktor untersucht. Nach Anregung der C—F-Streckschwingung (ν_3) in CH_3F bei niedrigen Drücken (10 m Torr) mit der P(20)-Linie bei 9,55 μm eines gepulsten CO_2 -Lasers (Laserleistung 10^5 – 10^6 W/cm²) konnte anhand der Fluoreszenz der C—H-Streckschwingung (ν_1, ν_4) bei 3,3 μm gezeigt werden, daß eine direkte Beobachtung der modenspezifischen Infrarotfluoreszenz nach Mehrphotonenabsorption im Bereich der Stoßzeiten der Moleküle möglich ist. Die Besetzung höherer Schwingungszustände erfolgt dabei um etwa zwei Größenordnungen rascher als durch Schwingungsenergieübertragung. — Durch zeitaufgelöste Beobachtung der Atom-Konzentration nach der Laseranregung war eine Unterscheidung zwischen reaktiven und energieübertragenden Prozessen möglich. Bei Zusatz von H- und D-Atomen wurde kein beschleunigter Verbrauch von CH_3F in den Schwingungszuständen $2\nu_3, \nu_1, \nu_4$ gefunden. Für die Geschwindigkeitskonstante der Reaktion



erhält man als obere Grenze

$$k_{1'} \leq 9 \cdot 10^9 \text{ cm}^3 \text{ mol}^{-1} \text{ s}^{-1} \text{ bei } 298 \text{ K}.$$

Bei O-Atomen wird eine effektive Schwingungsdesaktivierung beobachtet.



$$k_{2'a} \leq 10^{8.9} \text{ cm}^3 \text{ mol}^{-1} \text{ s}^{-1}$$

$$k_{2'b} = (8,0 \pm 1,6) \cdot 10^{11} \text{ cm}^3 \text{ mol}^{-1} \text{ s}^{-1} \text{ bei } 298 \text{ K}.$$

The effect of selective vibrational excitation on reactions of polyatomic molecules in the gas phase was investigated for the reaction of $\text{CH}_3\text{F}(v)$ with H-, D-, and O-atoms using the laser-induced fluorescence method combined with a discharge-flow reactor. After excitation of the ν_3 C—F-stretch vibration in CH_3F at low pressures (10 mTorr) with the P(20) line at 9.55 μm of a pulsed CO_2 -laser (intensity 10^5 – 10^6 W/cm²) detection of the fluorescence from C—H-stretch vibration (ν_1, ν_4) at 3.3 μm allows a direct observation of multiphoton excitation within the collision time of the molecules. The population of higher vibrational levels occurs about two orders of magnitude faster as expected from the rates of vibrational energy transfer. A distinction between reactive and inelastic processes was possible by a time-resolved observation of the atom concentration after the laser excitation. The addition of H- and D-atoms showed no effect on the decay rates of vibrationally excited CH_3F molecules. For the rate constant of the reaction



*) Teilweise Diplomarbeit M. Kneba, Göttingen 1974.